JOURNAL OF SOLID STATE CHEMISTRY 41, 185–194 (1982)

Electrical Conductivity in Calcium Titanate*

U. BALACHANDRAN, B. ODEKIRK, AND N. G. EROR

Oregon Graduate Center, 19600 Northwest Walker Road, Beaverton, Oregon 97006

Received August 3, 1981; in revised form October 7, 1981

The electrical conductivity of polycrystalline $CaTiO_3$ was measured over the temperature range 800–1100°C while in thermodynamic equilibrium with oxygen partial pressures from 10^{-22} to 10^{0} atm. The data were found to be proportional to the $-1/6$th power of the oxygen partial pressure for the oxygen pressure range 10^{-16}–10^{-22} atm, proportional to $P_{O_2}^{-1/4}$ for the oxygen pressure range 10^{-8}–10^{-15} atm, and proportional to $P_{O_2}^{+1/4}$ for the oxygen pressure range greater than 10^{-4} atm. The region of linearity where the electrical conductivity varies as $-1/4$th power of P_{O_2} increased as the temperature was decreased. The observed data are consistent with the presence of small amounts of acceptor impurities in $CaTiO_3$. The band-gap energy (extrapolated to zero temperature) was estimated to be 3.46 eV.

Introduction

In view of the important role played by alkaline earth titanates in ferroelectric and ferromagnetic phenomena, a brief investigation of the electrical properties of polycrystalline calcium titanate prepared by the liquid mix technique was carried out. $CaTiO_3$ has an orthorhombic structure at room temperature (*1*), and the structure becomes tetragonal at 600°C and cubic at 1000°C (*2*). From the optical density studies on single-crystal $CaTiO_3$, Linz and Herrington (*3*) determined the band-gap energy of 3.4 eV (at 0°K). They found that the absorption characteristics are quite similar to those of $SrTiO_3$ with the exception that the absorptions are shifted to shorter wavelengths.

Cox and Tredgold (*4*) measured the electrical conductivity of single-crystal $CaTiO_3$ at 130°C and reported to be p-type, presumably after exposure to oxidizing atmospheres. Thermopower measurement also indicated that electron holes are the majority carriers. It should be pointed out that the conductivity measurements at 130°C may not be reliable—the conductivity of the oxidized material must be less than 10^{-10} ohm^{-1} cm^{-1}. George and Grace (*5*) examined the electrical conductivity and Seebeck coefficient of $CaTiO_3$ in water-hydrogen atmospheres from 1100 to 1300°C. They concluded that an oxygen vacancy model was applicable to their results. George and Grace (*6*) investigated the diffusion of point defects in $CaTiO_3$. The reported studies on $CaTiO_3$ indicate that there is an extensive range of low oxygen partial pressures (P_{O_2}), where the conductivity increases with decreasing P_{O_2}, characteristic of n-type conduction related to oxygen deficiency. Walters and Grace (*7*) studied the electrical conductivity and Seebeck coefficient of $SrTiO_3$ in damp hydrogen mixtures for a narrow range of oxygen partial pressure. Recently Balachan-

* This research was sponsored by the Gas Research Institute.

0022-4596/82/020185-10$02.00/0

dran and Eror (*8*) investigated the electrical conductivity of polycrystalline $SrTiO_3$ in the P_{O_2} range of 10^0 to 10^{-22} atm and temperature range of 800 to 1050°C. The structural analog $BaTiO_3$ has been studied in much detail in both the polycrystalline (*9–14*) and single-crystal (*15*) states. All these studies on $BaTiO_3$ and $SrTiO_3$ indicate that in the P_{O_2} range near 1 atm, the conductivity increases with increasing P_{O_2}, characteristic of p-type conduction related to a stoichiometric excess of oxygen. $CaTiO_3$, however, has not been studied at elevated temperatures while in equilibrium with P_{O_2} near 1 atm.

In the present study, the high-temperature equilibrium electrical conductivity of polycrystalline $CaTiO_3$ has been measured as a function of P_{O_2} in the range 10^0–10^{-22} atm. By matching the observed electrical characteristics to specific defect models the predominant defect structures are identified.

Experimental

The specimens employed in this investigation were prepared by a liquid mix technique (*16, 17*). Required amounts of calcium carbonate (Mallinckrodt Chemical Works) and tetraisopropyl titanate solution (Tyzor, Dupont Co.) were dissolved in an ethylene glycol–citric acid solution. There was no evidence of any precipitation in the solutions as they were evaporated to a rigid transparent, uniformly colored polymeric glass. The glass retains homogeneity on an atomic scale and was calcined at 900°C—there was no evidence of a second phase in the as-calcined samples. These powder samples were pressed into thin circular disks (1.2 cm in diameter and 0.1 cm thick) under a load of 40,000 psi, and sintered in air at 1350°C for 12 hr. The density of the sintered disks was 94% of the theoretical density. Conductivity specimens were cut from this sintered disk using an airbrasive unit. The specimens were wrapped with four 0.025-cm platinum wires as described in the literature (*18, 19*). Small notches were cut in the edges of the sample to aid in holding the platinum wires in place.

A conventional four-probe direct-current technique was employed for all electrical conductivity measurements. The four platinum leads were insulated from one another by recrystallized high-purity alumina insulators. A standard taper Pyrex joint to which capillary tubes had been sealed was mounted on top of the furnace reaction tube assembly. The platinum wires exited through the capillary tubes and were glass sealed vacuum tight into the tubes.

The oxygen partial pressures surrounding the samples were controlled by flowing metered mixtures of gases past the sample. The gases were oxygen, compressed air, argon with known amounts of oxygen, CO_2/CO mixtures, and CO_2/H_2 mixtures. The error in volumetric ratio measurements of CO_2/CO mixtures resulted in an error of about 1% in the P_{O_2} value reported here. The conductivity was measured as a function of P_{O_2} in the temperature range 800–1100°C. The conductivity was determined by measuring the voltage across the potential probes using a high-impedance ($>10^{10}$ ohm) digital voltmeter (Keithley 191 Digital Multimeter). The current was supplied between the two outer leads by a constant-current source (Keithley 225 current source). The voltage was measured with the current in both forward and reverse directions, and the conductivity was calculated from the average values. After each variation of the gas atmosphere surrounding the sample the conductivity was measured as it changed to the new equilibrium value. The process of change in conductivity was recorded and if the conductivity no longer changed, it was assumed that the state of equilibrium had been attained. This state proved to be attainable reversibly from higher or lower oxygen partial pres-

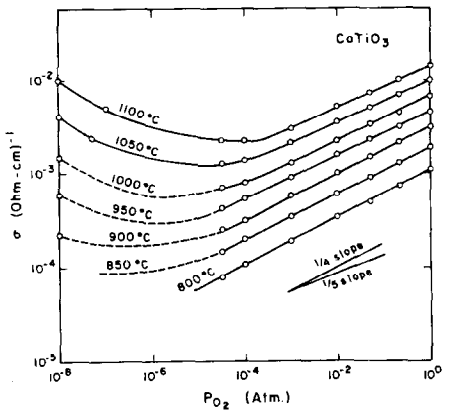

FIG. 1. The electrical conductivity of polycrystalline $CaTiO_3$ as a function of oxygen partial pressure at constant temperature, from 10^{-8} to 10^{0} atm.

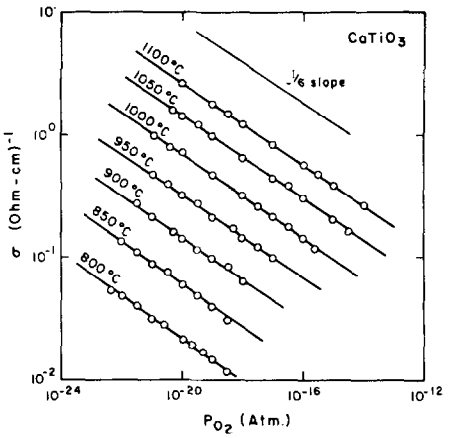

FIG. 2. The electrical conductivity of polycrystalline $CaTiO_3$ as a function of oxygen partial pressure at constant temperature, from 10^{-22} to 10^{-15} atm.

sures. Equilibrium was established as fast as the oxygen pressure could be changed from one value to another (which is usually less than 15 min). Current was varied from 20 μA to 1 mA and no significant change in electrical conductivity was observed. Changing the ratio of the surface area to the volume by varying the size and geometry of the samples produced no detectable difference in the measured conductivity which indicated that the measured quantity was the bulk conductivity.

Results and Discussion

The electrical conductivity of polycrystalline $CaTiO_3$ in the temperature range 800–1100°C and in equilibrium with oxygen partial pressures between 10^{-8} and 10^{0} atm is shown in Fig. 1. As can be seen, the conductivity shifts from p-type to n-type as P_{O_2} is decreased. The n-type electrical conductivity of $CaTiO_3$ was extended to lower oxygen partial pressures by employing CO/CO_2 and H_2/CO_2 mixtures. The oxygen pressure dependence for conductivity changed from $-1/4$th to $-1/6$th power as the P_{O_2} is decreased in the n-type region and the different regions are treated separately in the following text.

Region I ($P_{O_2} = 10^{-22}$–10^{-16} atm)

The variation of the electrical conductivity with oxygen partial pressure in this region is given in Fig. 2. The log σ vs log P_{O_2} data (see Fig. 2) are linear for as many as six decades of oxygen partial pressure for a given temperature (above 1000°C) and linear for four decades of P_{O_2} for temperatures in the range 800–950°C. This extensive region of linearity affords the opportunity to determine the defect model responsible for the n-type electrical conductivity in this region. A slope of approximately $-1/6$ is found for the log σ vs log P_{O_2} data (see Table I). This slope is similar to that found for $BaTiO_3$ (*12–15*) and $SrTiO_3$ (*7, 8*), as well as to the results of George and Grace (*5*) for single-crystal $CaTiO_3$ in the temperature range 1100–1300°C and P_{H_2O}/P_{H_2} ratios from 2×10^{-4} to 8×10^{-2}.

The variation of the electrical conductivity with the oxygen partial pressure is calculated in terms of the oxygen vacancy defect model. The basis for the calculation is the reaction that represents the formation of a doubly ionized oxygen vacancy $[V_O^{\cdot\cdot}]$ and two electrons available for conduction by the removal of an oxygen from a normal

TABLE I

P_{O_2} DEPENDENCE OF CONDUCTIVITY IN THE REGION 10^{-22}–10^{-16} atm

T (°C)	m for $\sigma_n \propto P_{O_2}^{-1/m}$
800	5.90
850	5.95
900	5.95
950	6.04
1000	5.95
1050	5.95
1100	5.90

lattice site into the gas phase. The reaction is

$$O_O^x \rightleftharpoons \tfrac{1}{2} O_2 + V_O^{\cdot\cdot} + 2e'. \quad (1)$$

The equilibrium constant for reaction (1) is

$$K_1 \cong [V_O^{\cdot\cdot}]\,[n]^2\,P_{O_2}^{1/2} = \exp\left(\frac{-\Delta G_f}{RT}\right), \quad (2)$$

where $[n] \equiv [e']$. With two electrons resulting from each oxygen vacancy, it follows that

$$[n] \cong 2\,[V_O^{\cdot\cdot}]. \quad (3)$$

Expressing the free energy change in terms of the enthalpy change, ΔH_f, and entropy change, ΔS_f, and substituting Eq. (3) into Eq. (2), the result for the electron concentration is

$$[n] = 2^{1/3} P_{O_2}^{-1/6} \exp\left[\frac{\Delta S_f}{3R}\right] \exp\left[\frac{-\Delta H_f}{3RT}\right], \quad (4)$$

and the electrical conductivity, σ, is given by

$$\sigma = 2^{1/3}\,P_{O_2}^{-1/6}\,e^{\mu} \exp\left[\frac{\Delta S_f}{3R}\right] \exp\left[\frac{-\Delta H_f}{3RT}\right], \quad (5)$$

where e is the electronic charge, and μ is the mobility of the conduction electrons. At constant temperature, assuming that the mobility is independent of the change in concentration of oxygen vacancies, a plot of the logarithm of the electrical conductivity vs the logarithm of the P_{O_2} should result in a straight line with a slope of $-1/6$. The data in Fig. 2 and Table I are in good agreement with the predicted $-1/6$ dependence.

An indication of the magnitude of ΔH_f, the enthalpy of the oxygen extraction reaction, Eq. (1), is typically obtained from Arrhenius plots of the conductivity, as deduced from Eq. (5). This procedure neglects contributions from the temperature dependences of the carrier mobility or density of states. The values of ΔH_f calculated from the slope of the Arrhenius plots in Fig. 3 are listed in Table II. An average value of 5.99 eV (138.18 kcal/mole) is estimated for ΔH_f. George and Grace (*5*) obtained a value of 6.55 eV. Balachandran and Eror (*8*) determined a value for ΔH_f of 4.85 eV for polycrystalline $SrTiO_3$ in this region. It must be pointed out, however, that in view of the lack of knowledge regarding the temperature dependence of the electron mobility, such estimation of the value of ΔH_f must be taken with caution. No anomalous behavior is observed while

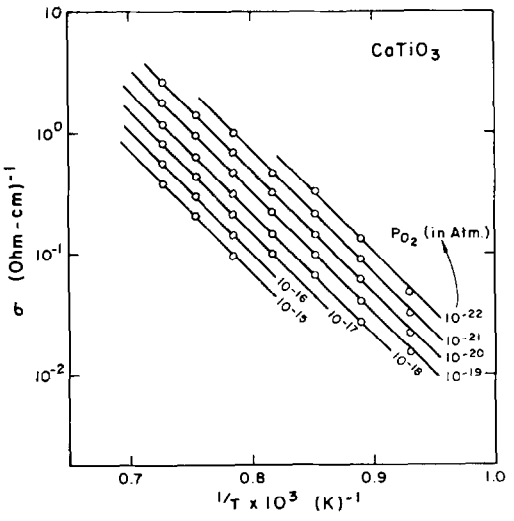

FIG. 3. Temperature dependence of electrical conductivity in polycrystalline $CaTiO_3$ in the P_{O_2} region 10^{-22}–10^{-15} atm.

TABLE II

ACTIVATION ENTHALPIES FOR CONDUCTION IN THE REGION 10^{-22}–10^{-16} atm

P_{O_2} (atm)	Activation enthalpy (kcal/mole)
10^{-22}	137.19
10^{-21}	138.90
10^{-20}	138.90
10^{-19}	137.30
10^{-18}	137.30
10^{-17}	138.80
10^{-16}	138.90

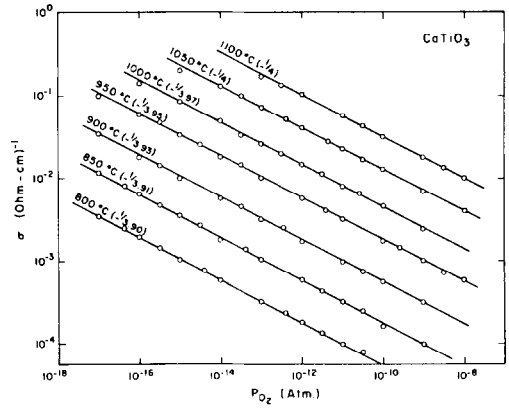

FIG. 4. The electrical conductivity of polycrystalline $CaTiO_3$ as a function of oxygen partial pressure at constant temperature, from 10^{-17} to 10^{-8} atm.

measuring the electrical conductivity in the temperature range 800–1100°C, indicating that the tetragonal to cubic phase transition at ~1000°C has apparently no effect on the measured conductivity at these temperatures.

Region II ($P_{O_2} = 10^{-8}$–10^{-15} atm)

A slope of ~1/4 is found for the log σ vs log P_{O_2} data (Fig. 4). Balachandran and Eror (*8*) observed a slope of approximately $-1/4$ from their log σ vs log P_{O_2} plot for $SrTiO_3$ in the P_{O_2} range 10^{-8}–10^{-15} atm and attributed it to the presence of small amounts of unknown acceptor impurities in the undoped $SrTiO_3$ sample. For the case of undoped $BaTiO_3$ prepared by the same technique as that used here, Chan and Smyth (*14*) reported a net acceptor impurities about 130 ppm (atomic). They proposed that all undoped material ($BaTiO_3$) studied to date had a net excess of acceptor impurities, and attributed this to the fact that potential acceptor elements are naturally much more abundant than potential donor elements. We believe that our samples also contained some unknown acceptor impurities.

In discussing the concept of the impurity effect, it is helpful to consider a Kröger–Vink (*20*) diagram for a ternary oxide of the type ABO_3 with an acceptor impurity. We will, for the purpose of illustration, consider Schottky–Wagner disorder to describe the nonstoichiometry. Figure 5 illustrates the variation of defect concentrations as a function of oxygen partial pressure for the case of fully ionized atomic defects, electrons $[n]$, and electron holes $[p]$ in a pure ternary oxide ABO_3 with both A and B site vacancies. It is assumed that the A and B content of the oxide is constant. Complete thermodynamic definition of a ternary oxide in equilibrium with only one crystal component, e.g., oxygen, requires the specification of three thermodynamic variables according to the phase rule. If both cationic species are sufficiently nonvolatile, the atomic ratio of the cations, A/B, whether known, or unknown but assumed constant, can be considered adequate in addition to temperature and total pressure while equilibrating with oxygen (*21*). The familiar $[n] \propto P_{O_2}^{-1/6}$ in the region with charge neutrality condition $[n] \approx 2[V_O^{\cdot\cdot}]$ is illustrated in Fig. 5. In Fig. 6, an acceptor impurity, I_m, is added that is always fully ionized, I_m', to the ternary oxide ABO_3. In Fig. 6 note that for sufficient departures from stoichiometry it may be possible for the electrical conductivity to be controlled by $[n] \approx 2[V_O^{\cdot\cdot}]$ and to thereby mask the

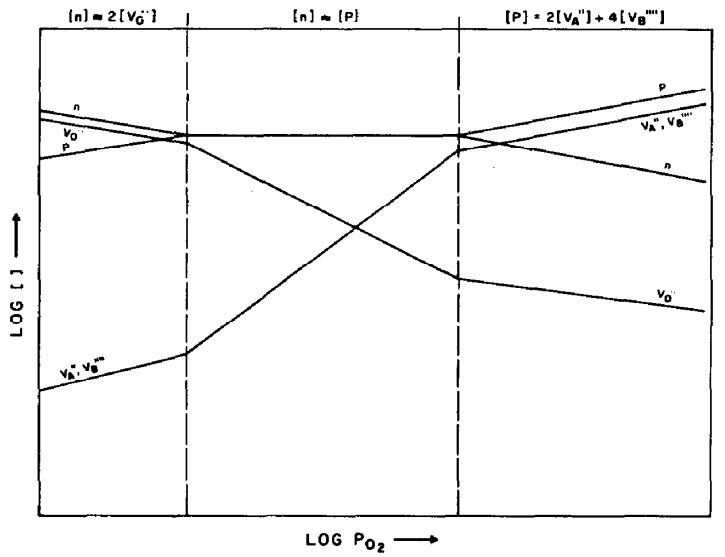

FIG. 5. Defect concentration vs the oxygen pressure in the ternary oxide of the type ABO_3 with Schottky–Wagner disorder.

effect of the acceptor impurity. The two major points to be derived from Fig. 6 are that the electronic n to p transition has been shifted to lower oxygen partial pressures and the metal-excess to metal-deficit transition has been shifted to higher oxygen partial pressures when an acceptor impurity is added to ABO_3.

In Fig. 6, there is a region with electrical neutrality condition $[I_m'] \approx 2\,[V_O^{\cdot\cdot}]$ in which the electron concentration varies as the $-1/4$th power and the electron hole con-

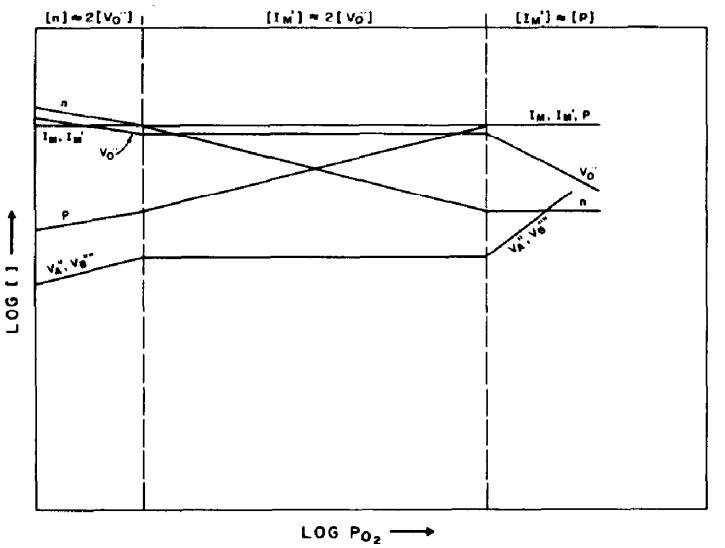

FIG. 6. Logarithm of the defect concentration for the ternary oxide ABO_3 with a fully ionized acceptor impurity, I_m, and Schottky–Wagner disorder as a function of logarithm of oxygen pressure.

centration increases as the +1/4th power of oxygen partial pressure. In this region, for certain values of P_{O_2}, the electron concentration is greater than electron hole concentration and, hence, the conductivity is n-type with a −1/4th dependence on P_{O_2}. As the oxygen partial pressure increases, the electron hole concentration becomes greater than the electron concentration after a certain value of P_{O_2} and the material becomes p-type with a +1/4th dependence for conductivity on P_{O_2}. When the P_{O_2} value is increased further, the electron hole concentration becomes equal to the acceptor concentration, which is constant, and, hence, the electrical conductivity is independent of P_{O_2}, with the charge neutrality condition $[I'_m] \approx [p]$ as shown in Fig. 6.

The observed slope of $\sim -1/4$ from the $\log \sigma$ vs $\log P_{O_2}$ data (Fig. 4) in this region of P_{O_2} is interpreted in terms of the presence of accidental acceptor impurities, such as Fe, Al, or Cr on Ti sites. Thus, the condition of charge neutrality in this region can be

$$[I'_m] \approx 2\,[V_O^{\cdot\cdot}]. \tag{6}$$

With this neutrality condition and Eqs. (1) and (2), the electrical conductivity varies with oxygen partial pressure as shown in

$$\sigma = 2^{1/2} \frac{1}{[I'_m]^{1/2}} P_{O_2}^{-1/4} e\mu \times \exp\left[\frac{\Delta S_f}{2R}\right] \exp\left[\frac{-\Delta H_f}{2RT}\right]. \tag{7}$$

The slopes of the lines drawn in Fig. 4 are in excellent agreement with the predicted value of −1/4 by the above impurity model. The activation enthalpies of conduction derived from the Arrhenius slopes (see Fig. 7) are shown in Table III. An average value of 5.16 eV (118.90 kcal/mole) is estimated for this region.

Transition Region

Becker and Frederikse (*22*) showed that the band-gap energy (extrapolated to zero temperature) of a semiconductor which exhibits a p to n transition may be determined from the Arrhenius plots of the conductivity minima. The $\log \sigma_{min}$ vs $1/T$ data in Fig. 8 indicate a value E_g° = 3.46 eV (79.79 kcal/mole) as the band gap for the polycrystalline $CaTiO_3$ extrapolated to 0°K.

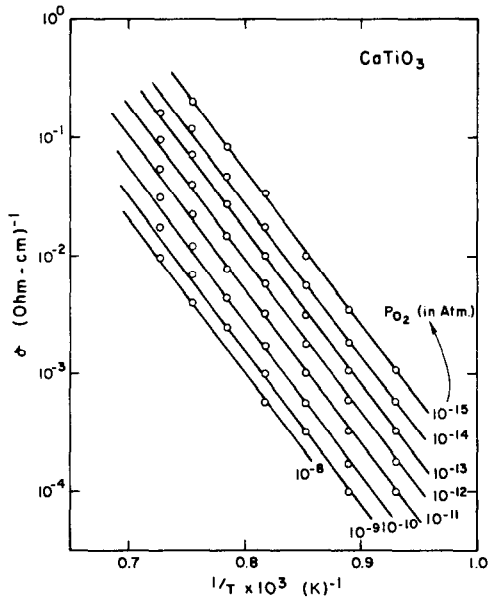

FIG. 7. Temperature dependence of conductivity of polycrystalline $CaTiO_3$ in the P_{O_2} region 10^{-15}–10^{-8} atm.

TABLE III

ACTIVATION ENTHALPIES FOR CONDUCTION IN THE REGION 10^{-15}–10^{-8} atm

P_{O_2} (atm)	Activation enthalpy (kcal/mole)
10^{-15}	118.90
10^{-14}	117.75
10^{-13}	120.61
10^{-12}	118.90
10^{-11}	118.30
10^{-10}	118.90
10^{-9}	118.90
10^{-8}	118.90

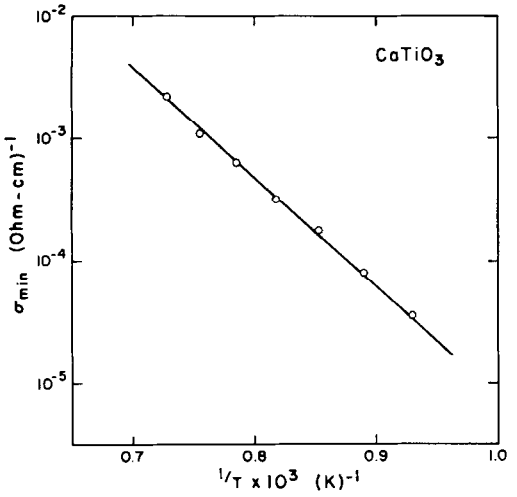

FIG. 8. Temperature dependence of the conductivity minimum of polycrystalline $CaTiO_3$.

This is in good agreement with the range of values 3.2–3.4 eV reported from optical absorption data (*3, 4, 23*) on single-crystalline $CaTiO_3$. Extrapolation was used to obtain a continuous plot for the log σ vs log P_{O_2} data in the entire oxygen partial pressure range used in this work and from these plots the conductivity minima in the temperature range 800–1000°C were obtained. Frederikse *et al.* (*24*) found a band-type conduction process in the structural analog $SrTiO_3$. Assuming a band-type conduction model for $CaTiO_3$, the full expression for the log σ_{min} vs $1/T$ plot is

$$\frac{\partial \ln \sigma_{min}}{\partial (RT)^{-1}} = \frac{\partial}{\partial (RT)^{-1}} \left[\frac{\ln \mu_n \mu_p}{2} + \ln N_c N_v \right] - \frac{E_g^\circ}{2}, \quad (8)$$

where N_c and N_v are the density of states near the conduction and valence band edges, respectively. Assuming that the temperature dependence of the mobilities is the same for electrons and electron holes, and if both N_c and N_v are proportional to $T^{+3/2}$, mobility and density of state terms cancel each other, and the Arrhenius slope is directly proportional to E_g°.

p-Type Region ($P_{O_2} > 10^{-4}$ atm)

The conductivity data obtained in the range $10^{-8} < P_{O_2} < 1$ atm are shown in Fig. 1. The conductivity in the region of P_{O_2} greater than 10^{-4} atm increases with increasing oxygen partial pressure, indicative of p-type, or oxygen-excess, conductivity. The region of linearity in the p-type region increases in width with decreasing temperature as the p–n transition moves to lower P_{O_2}. The slopes of the oxygen pressure dependence for conductivity given in Table IV indicate that the values are tending toward 1/4 with decreasing temperature where the range of linearity is greatest. Arrhenius plots of the data at constant oxygen pressure are shown in Fig. 9, and the activation enthalpies of conduction derived from the slopes are given in Table V. A value of about 2.16 eV (49.84 kcal/mole) appears to be typical. Balachandran and Eror (*8*) obtained a value of 1.59 eV (36.7 kcal/mole) in the p-type region for $SrTiO_3$.

It is apparent that a stoichiometric excess of oxygen can be incorporated into the $CaTiO_3$ lattice by a remarkably favorable process. In contrast to the value of 2.16 eV obtained in this work, enthalpies of oxygen addition for a large number of rare earth and alkaline earth oxides are of the order of 3–6 eV (*25*).

It has been shown in $BaTiO_3$ (*11, 14, 15*)

TABLE IV

P_{O_2} DEPENDENCE OF CONDUCTIVITY FOR THE P-TYPE REGION

T (°C)	m for $\sigma_p \propto P_{O_2}^{+1/m}$
800	4.00
850	4.05
900	4.00
950	4.20
1000	4.28
1050	4.50
1100	4.50

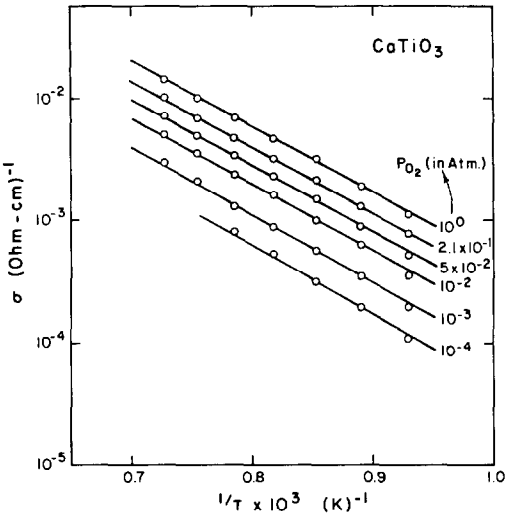

FIG. 9. Temperature dependence of the conductivity of polycrystalline $CaTiO_3$, in the p-type region.

and $SrTiO_3$ (*8*) that the p-type conductivity arises from the incorporation of oxygen into the impurity-related oxygen vacancies, where the reaction is

$$[V_o^{\cdot\cdot}] + \tfrac{1}{2}\,O_2 \rightleftharpoons O_o^x + 2h. \qquad (9)$$

The condition of charge neutrality in the near-stoichiometric region is the same as that observed in region II, i.e.,

$$[I_m'] \approx 2\,[V_o^{\cdot\cdot}].$$

The chemical mass action expression for Eq. (9) is

$$\frac{[p]^2}{[V_o^{\cdot\cdot}]} = K_9 P_{O_2}^{1/2} = K_9' P_{O_2}^{1/2} \exp\left(\frac{-\Delta H_p}{RT}\right). \qquad (10)$$

Combination of Eq. (6) with Eq. (10) gives

$$[p] = \left(\frac{K_9'\,[I_m']}{2}\right)^{1/2} P_{O_2}^{1/4} \exp\left(\frac{-\Delta H_p}{2RT}\right). \qquad (11)$$

This gives

$$\sigma \propto P_{O_2}^{1/4} \qquad (12)$$

TABLE V

ACTIVATION ENTHALPIES FOR CONDUCTION IN THE p-TYPE REGION

P_{O_2} (atm)	Activation enthalpies (kcal/mole)
10^0	49.84
2.1×10^{-1}	50.30
5.0×10^{-2}	49.16
10^{-2}	49.16
10^{-3}	50.30
10^{-4}	50.30

as observed, as long as only a minor fraction of the impurity-related $V_o^{\cdot\cdot}$ is filled. The trend toward shallower slopes at higher temperatures represents an intrusion of the transition region leading to the conductivity minima which are moving toward higher P_{O_2} with increasing temperature. The ready availability of oxygen vacancies explains the unusual ease with which the material accepts a stoichiometric excess of oxygen.

The estimated acceptor impurity in our sample is approximately 400 ppm. These impurities and their charge-compensating partner, $V_o^{\cdot\cdot}$, dominate the charge neutrality condition in a wide range of P_{O_2} ($>10^{-16}$ atm). Impurity-insensitive behavior is observed in the range of lowest P_{O_2}, where the electrical conductivity varies as $P_{O_2}^{-1/6}$.

The pressure and temperature dependences, as well as the absolute values of the electrical conductivity, obtained in this study agree very well with the values (at 1100°C) reported by George and Grace (*5*) in single-crystal $CaTiO_3$ in the impurity-insensitive region. This agreement between the polycrystalline sample used in this investigation and the single crystal used by George and Grace (*5*) indicates that grain boundaries have no significant effect on the electronic transport in this range of experimental conditions, even though the grain boundaries often play an important role in determining the physical properties of polar

crystalline solids at ordinary temperatures (*26*).

Conclusions

The experimental results agree well with the predictions based on the doubly ionized oxygen vacancy defect model, Eq. (1), at the lowest P_{O_2} and temperature range 800–1100°C. The P_{O_2} region in which the doubly ionized oxygen vacancies are dominant defects becomes narrow as the temperature is decreased. The logarithm of the electrical conductivity is a linear function of the logarithm of P_{O_2} at constant temperature with a slope of $-1/6$ and this agrees with the predicted value.

The defect chemistry of undoped $CaTiO_3$ is dominated by accidental acceptor impurities and their related oxygen vacancies, Eq. (6), for $P_{O_2} > 10^{-16}$ atm. Because of the acceptor impurities, a region in which the conductivity varies as the $-1/4$th power of oxygen partial pressure is observed. Intrinsic ionic disorder never plays a significant role because of the high ionic charges and the lack of suitable interstitial sites. The band gap is sufficiently high (3.46 eV) to keep intrinsic electronic disorder below the net acceptor impurity content of the material.

The p-type behavior observed in the region $P_{O_2} > 10^{-4}$ atm results from incorporation of oxygen into the impurity-related oxygen vacancies, Eq. (9). The ready availability of oxygen vacancies results in low enthalpy for the oxygen incorporation reaction.

Acknowledgement

The authors wish to thank the Gas Research Institute for financial support in carrying out this investigation.

References

1. H. F. KAY AND P. C. BAILEY, *Acta Crystallogr.* **10,** 219 (1957).
2. H. F. KAY, Report, Brit. Elec. Res. Assoc., Ref. LT 257 (1951).
3. A. LINZ AND K. HERRINGTON, *J. Chem. Phys.* **28,** 824 (1958).
4. G. A. COX AND R. H. TREDGOLD, *Brit. J. Appl. Phys.* **18,** 37 (1967).
5. W. L. GEORGE AND R. E. GRACE, *J. Phys. Chem. Solids* **30,** 881 (1969).
6. W. L. GEORGE AND R. E. GRACE, *J. Phys. Chem. Solids* **30,** 889 (1969).
7. L. C. WALTERS AND R. E. GRACE, *J. Phys. Chem. Solids* **28,** 239 (1967).
8. U. BALACHANDRAN AND N. G. EROR, *J. Solid State Chem.* **39,** 351 (1981).
9. H. VEITH, *Z. Angew. Phys.* **20,** 16 (1965).
10. F. FOSEK AND H. AREND, *Phys. Status Solidi* **24,** K69 (1967).
11. S. A. LONG AND R. N. BLUMENTHAL, *J. Amer. Ceram. Soc.* **54,** 515 (1971).
12. S. A. LONG AND R. N. BLUMENTHAL, *J. Amer. Ceram. Soc.* **54,** 577 (1971).
13. A. M. J. H. SEUTER, *Philips Res. Rep. Suppl.* No. 3, 1 (1974).
14. N. H. CHAN AND D. M. SMYTH, *J. Electrochem. Soc.* **123,** 1585 (1976).
15. N. G. EROR AND D. M. SMYTH, *J. Solid State Chem.* **24,** 235 (1978).
16. M. PECHINI, U.S. Patent, 3,330,697, July 11, 1967.
17. N. G. EROR AND D. M. SMYTH, *in* "Chemistry of Extended Defects in Nonmetallic Solids" (L. Eyring and M. O'Keefe, Eds.), pp. 62–74, North-Holland, Amsterdam (1970).
18. S. P. MITOFF, *J. Chem. Phys.* **35,** 882 (1961).
19. J. B. PRICE AND J. B. WAGNER, *Z. Phys. Chem.* **49,** 257 (1966).
20. F. A. KRÖGER AND H. J. VINK, *Solid State Phys.* **3,** 307 (1956).
21. D. M. SMYTH, *J. Solid State Chem.* **16,** 73 (1976).
22. J. H. BECKER AND H. P. R. FREDERIKSE, *J. Appl. Phys.* **33,** 447 (1962).
23. L. A. HARRIS AND R. H. WILSON, *Annu. Rev. Mater. Sci.* **8,** 99 (1978).
24. H. P. R. FREDERIKSE, W. R. THURBER, AND W. R. HOSLER, *Phys. Rev. Sect. A* **134,** 442 (1964).
25. P. KOFSTAD, *in* "Nonstoichiometry, Diffusion and Electrical Conductivity in Binary Metal Oxides," Chaps. 11–12, Wiley, New York (1972).
26. E. H. GREENER AND W. M. HIRTHE, *J. Electrochem. Soc.* **109,** 600 (1962).